Journal of Virology

# Induced Maturation of Human Immunodeficiency Virus

**Simone Mattei, Maria Anders, Jan Konvalinka, Hans-Georg Kräusslich, John A. G. Briggs and Barbara Müller**

***J. Virol.*** **2014, 88(23):13722. DOI: 10.1128/JVI.02271-14.**
**Published Ahead of Print 17 September 2014.**

Updated information and services can be found at:
http://jvi.asm.org/content/88/23/13722

*These include:*

**REFERENCES** This article cites 59 articles, 23 of which can be accessed free at: http://jvi.asm.org/content/88/23/13722#ref-list-1

**CONTENT ALERTS** Receive: RSS Feeds, eTOCs, free email alerts (when new articles cite this article), more»

Information about commercial reprint orders: **http://journals.asm.org/site/misc/reprints.xhtml**
To subscribe to to another ASM Journal go to: **http://journals.asm.org/site/subscriptions/**

Journals.ASM.org

Downloaded from http://jvi.asm.org/ on November 6, 2014 by Uppsala Univ BMC

JVI Journals.ASM.org

# Induced Maturation of Human Immunodeficiency Virus

**Simone Mattei,[a,c] Maria Anders,[b] Jan Konvalinka,[d] Hans-Georg Kräusslich,[b,c] John A. G. Briggs,[a,c] Barbara Müller[b,c]**

Structural and Computational Biology Unit, European Molecular Biology Laboratory, Heidelberg, Germany[a]; Department of Infectious Diseases, Virology, University Hospital Heidelberg, Heidelberg, Germany[b]; Molecular Medicine Partnership Unit, Heidelberg, Germany[c]; Department of Biochemistry, Faculty of Science, Charles University in Prague, Prague, Czech Republic[d]

**ABSTRACT**

**HIV-1 assembles at the plasma membrane of virus-producing cells as an immature, noninfectious particle. Processing of the Gag and Gag-Pol polyproteins by the viral protease (PR) activates the viral enzymes and results in dramatic structural rearrangements within the virion—termed maturation—that are a prerequisite for infectivity. Despite its fundamental importance for viral replication, little is currently known about the regulation of proteolysis and about the dynamics and structural intermediates of maturation. This is due mainly to the fact that HIV-1 release and maturation occur asynchronously both at the level of individual cells and at the level of particle release from a single cell. Here, we report a method to synchronize HIV-1 proteolysis *in vitro* based on protease inhibitor (PI) washout from purified immature virions, thereby temporally uncoupling virus assembly and maturation. Drug washout resulted in the induction of proteolysis with cleavage efficiencies correlating with the off-rate of the respective PR-PI complex. Proteolysis of Gag was nearly complete and yielded the correct products with an optimal half-life ($t_{1/2}$) of ~5 h, but viral infectivity was not recovered. Failure to gain infectivity following PI washout may be explained by the observed formation of aberrant viral capsids and/or by pronounced defects in processing of the reverse transcriptase (RT) heterodimer associated with a lack of RT activity. Based on our results, we hypothesize that both the polyprotein processing dynamics and the tight temporal coupling of immature particle assembly and PR activation are essential for correct polyprotein processing and morphological maturation and thus for HIV-1 infectivity.**

**IMPORTANCE**

**Cleavage of the Gag and Gag-Pol HIV-1 polyproteins into their functional subunits by the viral protease activates the viral enzymes and causes major structural rearrangements essential for HIV-1 infectivity. This proteolytic maturation occurs concomitant with virus release, and investigation of its dynamics is hampered by the fact that virus populations in tissue culture contain particles at all stages of assembly and maturation. Here, we developed an inhibitor washout strategy to synchronize activation of protease in wild-type virus. We demonstrated that nearly complete Gag processing and resolution of the immature virus architecture are accomplished under optimized conditions. Nevertheless, most of the resulting particles displayed irregular morphologies, Gag-Pol processing was not faithfully reconstituted, and infectivity was not recovered. These data show that HIV-1 maturation is sensitive to the dynamics of processing and also that a tight temporal link between virus assembly and PR activation is required for correct polyprotein processing.**

Formation of infectious HIV-1 particles comprises (i) particle assembly at the plasma membrane, (ii) release of an immature virus by abscission of the viral lipid envelope from the host cell membrane, and (iii) proteolytic maturation which converts the particle into its infectious form (reviewed in references 1–3). The viral polyprotein Gag acts as key orchestrator of this sequence of events. It traffics to the cytosolic side of the plasma membrane, where it self-assembles into protruding virus buds. Gag also directs recruitment of the Gag-Pol polyprotein encoding the viral enzymes, the single-stranded RNA genome, and the Env glycoproteins to the viral budding site. Recruitment of the host cell endosomal sorting complex required for transport (ESCRT) machinery, mediated by the p6 domain of Gag, is required for virus bud abscission.

Newly formed virions comprise ~2,500 Gag and ~125 Gag-Pol molecules, organized into a truncated protein sphere lining the viral membrane. These so-called immature virions are noninfectious. During the process of virion maturation, the viral protease (PR), which is encoded as part of the *pol* open reading frame, cleaves Gag and Gag-Pol polyproteins into their mature subunits. This controlled proteolysis results in dramatic structural rearrangements within the particle (reviewed in references 1–3). In the mature virion, the matrix protein (MA) lines the viral membrane and the capsid protein (CA) forms the characteristic conical capsid encasing the RNA genome that is complexed and condensed by the nucleocapsid protein (NC) into a ribonucleoprotein complex (RNP). Proteolytic maturation and the ensuing morphological transitions of the viral architecture are essential for HIV-1 infectivity; the process activates the viral enzymes and converts the virion into a metastable form, ready for releasing the viral genome into a new target cell. Consequently, specific HIV-1 PR inhibitors

**Received** 5 August 2014 **Accepted** 11 September 2014
**Published ahead of print** 17 September 2014
**Editor:** F. Kirchhoff
Address correspondence to Barbara Müller, Barbara_Mueller@med.uni-heidelberg.de, or John A. G. Briggs, john.briggs@embl.de.
S.M. and M.A. contributed equally to this study.
Copyright © 2014, American Society for Microbiology. All Rights Reserved.
doi:10.1128/JVI.02271-14

Downloaded from http://jvi.asm.org/ on November 6, 2014 by Uppsala Univ BMC

(PI) block HIV-1 replication and are a keystone of current antiretroviral therapy (reviewed in references 4–6).

Despite its crucial importance for HIV-1 replication and many years of intense studies, the complex pathway of HIV-1 polyprotein processing and maturation is still incompletely understood. Very basic questions regarding the timing and kinetics of the process, as well as the structural transitions involved, remain unanswered. Cryoelectron microscopy (cEM) and cryoelectron tomography (cET) studies have defined the architecture of the starting and endpoints of morphological maturation (7–11). In the immature virion, Gag molecules are arranged in a contiguous hexameric lattice covering ~2/3 of the membrane surface. Crucial intermolecular contacts are provided by CA, and small irregular defects allow for curvature of the Gag shell with one large gap derived from the abscission point. The mature capsid is a fullerene-type cone built from CA hexamers and pentamers (12, 13). Significant differences between the immature and mature hexameric lattice (14) and the fact that only half of the available CA molecules are involved in mature capsid formation (15) suggest that maturation involves disassembly of the immature protein layer, followed by CA reassembly into a mature cone. According to this model, HIV morphogenesis involves two distinct assembly reactions: immature virion formation and assembly of the mature capsid (reviewed in references 1–3).

It appears evident that such complex dissociation/association events, occurring within the confined space of the virion packed with Gag-Pol and Gag components at high micromolar and millimolar concentrations, respectively, require tight spatiotemporal control. This assumption is supported by results from numerous studies involving mutation of PR recognition sites, partial PR inhibition, or artificial enhancement of PR activity. Inhibition of PR activity and premature processing due to enhanced activation of the enzyme are detrimental for virus replication (16). An ordered sequence of PR cleavage events has been deduced from *in vitro* analyses (17–19); accordingly, mutational analyses revealed that even partial blocking of processing at individual sites impairs viral infectivity, and an ordered series of cleavage events within Gag is important for formation of a mature viral core (20–22; reviewed in reference 23).

Investigation of the dynamics and pathway of HIV-1 maturation on a molecular level in tissue culture is hampered by the fact that the assembly, release, and maturation of individual virions produced from an infected cell, as well as from multiple cells in an infected culture, occur asynchronously over a time period of several hours. This has prevented dissection of individual steps of the process based on ensemble measurements. Live-cell imaging of fluorescently labeled virus derivatives has furthered our understanding of HIV-1 assembly dynamics (reviewed in reference 24), but a corresponding readout for proteolytic maturation is lacking. Furthermore, spatial resolution of even the most advanced fluorescence microscopy techniques is insufficient to provide insight into intravirion structural transitions. In the case of other viruses, this obstacle has been overcome by experimental settings that allow preparation of immature virus particles and subject them to a triggering event, e.g., exposure to low pH, that ensures synchronous onset of maturation in the bulk particle population (25) (reviewed in reference 26). For HIV-1, such a system has not been developed. Earlier attempts using temperature-sensitive variants of PR or inhibitor washout did not result in PR activation (27–29) (our unpublished observations). Here, we have revisited an inhibitor washout strategy for HIV-1 PR induction within viral particles, showing that activation of PR *in situ* is possible. Detailed characterization of the resulting particles highlights the importance of processing dynamics for virion morphogenesis.

## MATERIALS AND METHODS

**Cell lines and plasmids.** HEK293T and TZM-bl cells were cultured in Dulbecco's modified Eagle's medium (DMEM; Invitrogen) supplemented with 10% fetal calf serum (FCS; Biochrom), penicillin (100 IU/ml), streptomycin (100 μg/ml), 4 mM glutamine, and 10 mM HEPES (pH 7.4). Proviral plasmid pNL4-3 (30) and its nonreplication competent derivative pCHIV (31) have been described. A PR-deficient variant of pCHIV was generated by exchanging the codon for the active-site aspartic acid (D25) of PR to the codon for asparagine by site-directed mutagenesis.

**Antisera and reagents.** Polyclonal rabbit antisera were raised against purified, recombinant HIV-1 MA, CA, reverse transcriptase (RT), and integrase (IN). Polyclonal goat antiserum against HIV-1 NC was a kind gift from J. Lifson (NCIFrederick, USA). Amprenavir (APV), atazanavir (ATV), darunavir (DRV), indinavir (IDV), lopinavir (LPV), ritonavir (RTV), tipranavir (TPV), and saquinavir (SQV) were obtained through the AIDS Research and Reference Reagent Program, Division of AIDS, NIAID. Compounds were dissolved as 10 mM stock solutions in 100% dimethyl sulfoxide (DMSO) and stored at −80°C.

**Inhibitor washout.** HEK293T cells were transfected with pNL4-3 or pCHIV, using polyethyleneimine, by following standard procedures. A final concentration of 5 μM the indicated PI or DMSO (control) was added at the time of transfection. At 44 h posttransfection (hpt), tissue culture supernatant was harvested and passed through a 0.45-μm nitrocellulose filter. Virus was pelleted by ultracentrifugation through a 20% (wt/wt) sucrose cushion (SW32, 28,000 rpm, 90 min, 4°C). Pellets were resuspended in 1 ml phosphate-buffered saline (PBS) lacking PI, and centrifugation through a sucrose cushion was repeated (100 μl 20% sucrose; TLA-55, 44,000 rpm, 45 min, 4°C). For structural analyses, additional purification was performed between the two pelleting steps by centrifugation through an iodixanol density gradient as described previously (32). Final samples were resuspended in proteolysis buffer (25 mM MES [pH 6.0], 150 mM NaCl, 1 mM EDTA, 5 mM dithiothreitol), and incubation at 37°C was performed for the indicated time periods. For exogenous PR digestion, particles resuspended in the same buffer were treated with 0.1% Triton X-100 for 5 min on ice, purified recombinant HIV-1 PR was added at the indicated concentrations, and samples were incubated at 37°C.

Virion-associated RT activity was determined by a Sybr green I PCR enhanced RT assay (SG-PERT) (33). Particle infectivity was determined by titration on TZM-bl indicator cells. At 44 h after infection, cell lysates were harvested and analyzed for HIV-1 Tat-driven reporter gene activity using a commercial luciferase assay system (SteadyGlo; Promega) by following the manufacturer's instructions. Data were analyzed using GraphPad Prism.

**Immunoblot analyses.** Samples were separated by SDS-PAGE (17.5%; 200:1 acrylamide-bisacrylamide) and transferred to nitrocellulose membranes by semidry blotting. Proteins were detected by polyclonal rabbit antiserum raised against purified recombinant HIV-1 MA, CA, RT, or IN. Secondary antibodies coupled to Alexa fluorescent dyes were used for detection with an Odyssey infrared imaging system as specified by the manufacturer (Li-Cor Biosciences, Lincoln, NE). Band intensities were quantitated using Image Studio Lite software (Li-Cor).

**Cryo-electron tomography.** Following a washout procedure as described above, samples were either incubated at 37°C overnight, followed by mild fixation with paraformaldehyde (1% PFA; 1 h at room temperature), or directly subjected to fixation. Samples were stored in aliquots at −80°C.

For tomography, samples were mixed with a solution of 10-nm gold beads and vitrified by plunge freezing for subsequent cEM. Images were collected on either an FEI Titan Krios or an FEI Tecnai F30 Polara, both equipped with a Gatan GIF 2002 post-column energy filter and a 2-k by

Downloaded from http://jvi.asm.org/ on November 6, 2014 by Uppsala Univ BMC

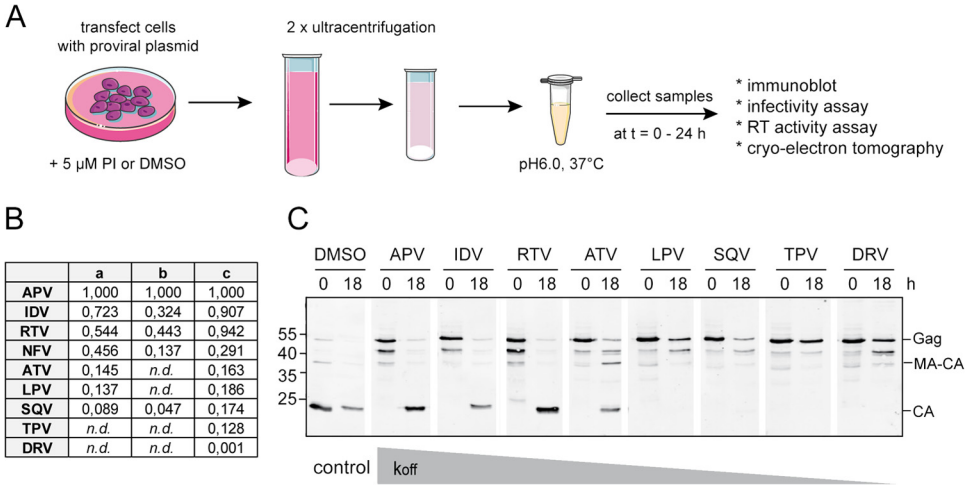


| | a | b | c |
|---|---|---|---|
| APV | 1,000 | 1,000 | 1,000 |
| IDV | 0,723 | 0,324 | 0,907 |
| RTV | 0,544 | 0,443 | 0,942 |
| NFV | 0,456 | 0,137 | 0,291 |
| ATV | 0,145 | *n.d.* | 0,163 |
| LPV | 0,137 | *n.d.* | 0,186 |
| SQV | 0,089 | 0,047 | 0,174 |
| TPV | *n.d.* | *n.d.* | 0,128 |
| DRV | *n.d.* | *n.d.* | 0,001 |

**FIG 1** Intravirion Gag processing following protease inhibitor washout. (A) Scheme of experiments performed in this study; (B) published off-rates for complexes between HIV-1 PR and a panel of PI determined by surface plasmon resonance measurements. The table summarizes data sets obtained under different experimental conditions reported by Shuman et al. (38) (a), Markgren et al. (37) (b), and Dierynck et al. (36) (c). Values shown were normalized to the off-rate value determined for APV in the respective study in order to facilitate comparison. *n.d.*, not determined. (C) 293T cells were transfected with pCHIV and grown in the presence of 5 μM the indicated PI. Tissue culture supernatants were harvested and subjected to an inhibitor washout procedure as described in Materials and Methods. Samples were either frozen (0) or incubated at pH 6.0 for 18 h (18), followed by immunoblot analysis using antiserum raised against HIV-1 CA. Numbers on the left of the blot are molecular masses in kDa.

2-k MultiScan charge-coupled-device (CCD) camera, both operated at 200 KeV. Images were acquired using the SerialEM software package (34) with a total dose of 15 electrons/Å$^2$ at a defocus of −4 or −7 μm. Tomographic tilt series were collected over an angular range of ±60° with a 3° step at a defocus of −6 μm using a total dose of ~50 electrons/Å$^2$. The nominal magnification for two-dimensional (2D) imaging and tomography was ×19,500 (pixel size of 4.3 Å) for the Titan Krios and ×34,000 (pixel size of 4.0 Å) for the Polara. Tomograms were reconstructed using the IMOD software package (35).

**Morphological analysis.** The 2D images were used to analyze the integrity and maturation state of a large number of particles from two independent preparations, while the 3D data from tomography were used to assess core morphology. Where necessary, to improve efficiency, low-magnification imaging was used to screen the EM grid and identify and select intact particles for tomography.

Each intact particle in the tomographic data sets was classified based on the morphology of the core structure, whether the core formed a closed shell or was partially open, and whether the RNP was encapsidated within the core or not. Morphology was classified as wild type (wt; containing the typical conical or tubular cores found in the wt viruses), mildly aberrant (cores with a slightly deformed structure with some similarity to the conical or tubular ones), or severely aberrant (cores with spherical or highly disordered core morphology).

## RESULTS

**Induction of Gag proteolysis by inhibitor washout.** HIV-1 maturation is efficiently inhibited by specific PR inhibitors (PI). Ten PI are currently in clinical use, all of which are reversible competitive inhibitors binding to the PR active site (5, 6). With the aim of establishing a system that allows controlled induction of HIV-1 proteolysis, we explored an inhibitor washout strategy as schematically outlined in Fig. 1A. For this, cells transfected with an HIV-1-expressing plasmid were grown in the presence of a specific PI. Tissue culture media containing immature virions were harvested, and the inhibitor was removed by repeated ultracentrifugation followed by immunoblot analysis of processing products.

We first tested a panel of clinically used PI. All PI used in antiviral therapy are efficient enzyme inhibitors characterized by low equilibrium dissociation constant ($K_D$) and $K_i$ values, but we reasoned that the potential for washout may be determined primarily by the off-rate of the PI rather than by its $K_i$ value. Kinetic binding parameters determined by surface plasmon resonance measurements using purified PR vary significantly between individual compounds, with off-rates differing by up to several orders of magnitude (36–38). Absolute rate constants and exact differences between off-rates vary between different studies employing different conditions and analysis setups, but the relative order of off-rates remains largely constant (summarized in Fig. 1B).

Following preparation of immature virions and inhibitor washout, samples were incubated in isotonic assay buffer for 18 h at 37°C. Purified HIV-1 PR is poorly active at neutral pH; optima in the range between pH 4.0 and 5.5 were determined for cleavage of small peptide substrates *in vitro* (39–41). Proteolysis of larger substrates comprising PR cleavage sites *in vitro* (42), as well as processing of Gag from virus-like particles by exogenously added recombinant HIV-1 PR (43), was found to be optimal at pH 6 to 7. We therefore chose mildly acidic buffer (pH 6.0) for our experiments.

No processing was observed following washout in the case of virions prepared in the presence of inhibitors characterized by comparatively slow off-rates (LPV, SQV, TPV, DRV) (Fig. 1C). In contrast, washout experiments with immature viruses prepared in the presence of APV, IDV, RTV, and ATV resulted in generation of mature CA. Relative band intensities revealed that the degree of Gag proteolysis roughly correlated with the relative off-rate of the respective inhibitor (Fig. 1B and C). Processing of Gag to CA was almost complete for washout experiments with APV, which exhibited the highest off-rate of all tested compounds (Fig. 1B and C) and was superior to the other clinically used PI (Fig. 1C) and to further experimental PI (data not shown). We thus selected APV for further experiments and employed SQV as a low-off-rate control.

Downloaded from http://jvi.asm.org/ on November 6, 2014 by Uppsala Univ BMC

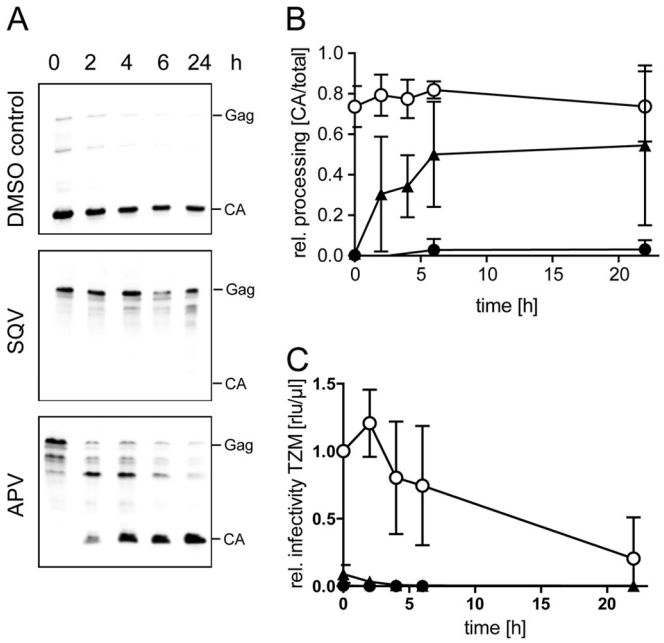


**FIG 2** Time course of induced Gag maturation. (A) 293T cells were transfected with pCHIV and grown in the presence of DMSO, APV, or SQV. Tissue culture supernatants were harvested and subjected to an inhibitor washout procedure as described in Materials and Methods. Samples were subsequently incubated at 37°C for the indicated time periods, followed by immunoblot analysis using antiserum raised against HIV-1 CA. (B) Relative degree of Gag processing. Band intensities for Gag, intermediate products, and CA were quantitated from immunoblot experiments as shown in panel A, and the proportion of mature CA to total CA reactive bands was calculated. The graph shows mean values and standard deviations (SD) from four independent experiments. Open circles, DMSO control; filled triangles, APV; filled circles, SQV. (C) Virus infectivity. Virus samples prepared and subjected to *in vitro* proteolysis for the indicated time periods were titrated on TZM-bl indicator cells, and infectivity was determined by quantitation of intracellular luciferase activity as described in Materials and Methods. Data were normalized to the respective DMSO control. The graph shows mean values and SD from five independent experiments. Open circles, DMSO control; filled triangles, APV; filled circles, SQV.

**Time course of induced Gag proteolysis.** In order to obtain an estimate for the time course of Gag proteolysis under our experimental conditions, particles produced in the presence of DMSO, APV, or SQV were subjected to inhibitor removal and incubated for different times at 37°C. PR was inactivated at the indicated time points by boiling of samples in SDS sample buffer, and the degree of Gag processing was assessed by immunoblotting (Fig. 2A). In accordance with the data shown in Fig. 1C, no substantial change in processing pattern over time was observed for the DMSO- or SQV-treated control samples. In contrast, a gradual transition from Gag to mature CA was observed over the 24-h incubation period following washout of the APV-treated sample (Fig. 2A). Quantitation of band intensities for mature CA relative to Gag and intermediate processing products was performed to obtain information on the time course of processing in this setup. While kinetics varied somewhat between experiments, an average half-life ($t_{1/2}$) of ~5 h for the formation of completely processed CA was estimated based on data from four independent experiments (Fig. 2B).

**Infectivity of particles obtained by induced proteolysis.** Complete processing to CA following APV washout and prolonged incubation *in vitro* suggested that this treatment may allow formation of mature infectious virus. We thus proceeded to test the infectivity of virions after induced processing by titration on reporter cells (Fig. 2C). Infectivity of control particles produced in the absence of PI (open circles) was not significantly affected by shorter incubation times (up to 5 h) and decreased 2- to 3-fold upon overnight incubation. APV-treated particles (filled triangles) displayed a very low residual infectivity at the beginning of the incubation period, while SQV-treated particles (filled circles) were completely noninfectious. No gain of infectivity was observed over the subsequent incubation period in either case, however, and the initial low infectivity of particles produced in the presence of APV was rapidly lost. Thus, despite full conversion of Gag into CA, no infectivity was recovered.

**Structural analysis of *in vitro* matured virions.** A possible explanation for the observed discrepancy between Gag processing and virus functionality is that formation of a full complement of completely processed CA subunits did not translate into assembly of a regular mature capsid structure. We therefore used cET to perform a detailed examination of particle morphology after induced proteolysis. Pooled results from two independent particle preparations for each condition are summarized in Fig. 3.

As expected, particles prepared in the presence of DMSO were found to be morphologically mature (Fig. 3Ai to iv); only a very small minority (~1%) displayed the typical immature truncated sphere morphology (Table 1). Incubation at 37°C for 20 h did not detectably alter virion architecture; virions fixed directly after washout and those subjected to further incubation were therefore pooled into a single population of DMSO control particles. Consistent with immunoblot results, particles prepared in the presence of APV exclusively showed the characteristic immature Gag lattice when analyzed directly after inhibitor washout without further incubation (Fig. 3Av and vi; Table 1). After 20 h of incubation of these particles at 37°C, only 7% of the imaged particles (18 of 257) retained an immature morphology (Table 1). The remaining particles had undergone structural maturation, but cET revealed defects in core morphology, closure, and encapsidation (Fig. 3Aviii to xii). The majority of cores (208 of 249) showed defects in morphology, most of these (61% of total) with severely aberrant phenotypes (Fig. 3B). In contrast, only 4% of cores (14 of 348) from DMSO-treated control particles were classified as severely aberrant and 15% (51 of 348) as mildly aberrant (Fig. 3B). A total of 58 of 249 (23%) cores from inhibitor-treated samples were not properly closed (Fig. 3Axi and xii), compared to only 5% (16 of 348) in the control sample (Fig. 3B). Furthermore, a condensed RNP was detected outside empty core structures in 80% (170 of 212) of particles from APV-treated samples (Fig. 3Aix, xi, and xii), compared to a minority (11%; 35 of 321) of particles in the control samples (Fig. 3B). A prototypic wild-type mature phenotype, characterized by a single, closed, conical capsid encasing a condensed RNP, was observed once after washout of the APV-treated sample (Fig. 3Avii).

**Induced processing of Gag and Gag-Pol products.** The results shown revealed that induced polyprotein processing led to normal amounts of fully processed CA, but formation of the mature capsid structure was severely impaired. An analogous phenotype has been observed before for HIV-1 derivatives carrying mutations at PR recognition sites in the C-terminal region of Gag (Fig. 4A, asterisks). Mutation of cleavage sites between NC, SP2, and p6 can affect HIV-1 infectivity and result in increased proportion of ab-

Downloaded from http://jvi.asm.org/ on November 6, 2014 by Uppsala Univ BMC

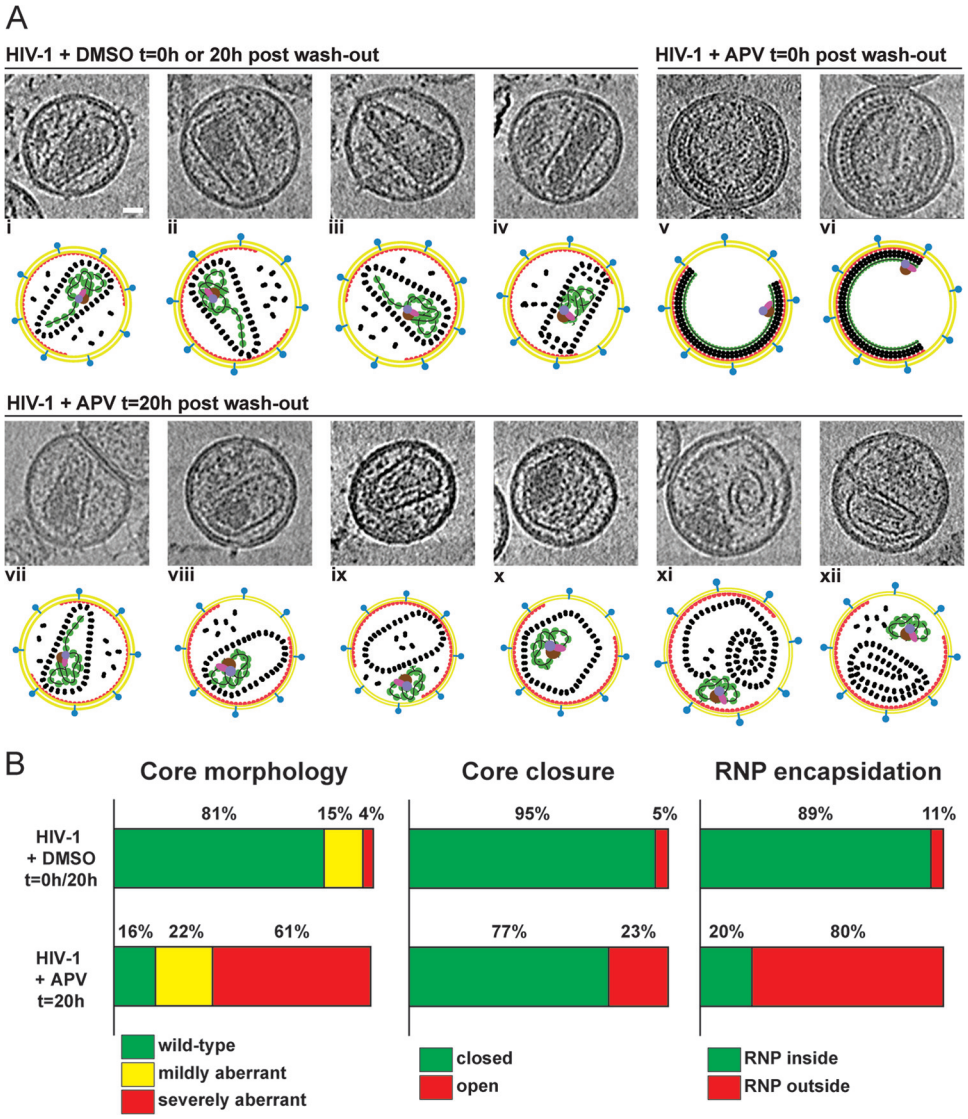


**FIG 3** Morphology of particles following *in vitro* maturation. (A) Gallery of typical particle morphologies, recorded from particles prepared under the indicated conditions. The figure depicts computational slices through tomograms. DMSO-treated controls show mainly characteristic mature particles with a conical or tubular closed core encasing the RNP density (i to iv). Particles analyzed immediately after APV washout showing the typical immature lattice (v and vi). (vii to xii) Examples of particles from APV washout subjected to 20 h of incubation. 3D tomograms were obtained for all intact particles that did not display an immature Gag layer at $t = 20$ h and classified according to the parameters indicated in panel B. Those illustrated here were classified as follows: wt, closed, RNP inside (vii); mildly aberrant, closed, RNP inside (viii); mildly aberrant, closed, RNP outside (ix); severely aberrant, closed, RNP inside (x); severely aberrant, open, RNP outside (xi and xii). Scale bar, 20 nm. (B) Statistical analysis of phenotypes. More than 150 particles obtained from two independent preparations were analyzed per condition. Statistical information based on 2D images of all particles recorded is summarized in Table 1.

**TABLE 1** Analysis of integrity and maturation state of the sample[a]

| Sample | Prep | Total no. of intact particles | Mature | | Immature | |
|---|---|---|---|---|---|---|
| | | | No. | % | No. | % |
| HIV and DMSO $t = 0$ h | | 331 | 327 | 99 | 4 | 1 |
| HIV and DMSO $t = 20$ h | 1 | 179 | 179 | 100 | 0 | 0 |
| | 2 | 95 | 91 | 96 | 4 | 4 |
| HIV and APV $t = 0$ h | 1 | 200 | 0 | 0 | 200 | 100 |
| | 2 | 200 | 0 | 0 | 200 | 100 |
| HIV and APV $t = 20$ h | 1 | 139 | 122 | 88 | 17 | 12 |
| | 2 | 118 | 117 | 99 | 1 | 1 |

[a] Data are based on 2D analysis of all particles recorded from the indicated virus preparation. *t* refers to the time of incubation at 37°C following the washout procedure.

errant capsid structures, even though the degree of CA processing is not impaired (20, 21, 44). We therefore performed a more comprehensive immunoblot analysis of Gag processing upon inhibitor washout using antibodies against MA and NC in addition to anti-CA (Fig. 4B). The appearance of fully processed MA (Fig. 4B, top) exactly paralleled the generation of CA (Fig. 4B, middle). NC was also converted to its fully processed form (Fig. 4B, bottom), but a higher proportion of incompletely processed NC-SP2 than DMSO-treated particles and a residual intermediate product likely representing NC-SP2-p6 (Fig. 4B, asterisk) remained after overnight incubation (Fig. 4B, bottom, compare lanes 6 and 7). Previous studies demonstrated that partial or even complete blocking of NC-SP2 processing does not significantly affect HIV-1

Downloaded from http://jvi.asm.org/ on November 6, 2014 by Uppsala Univ BMC

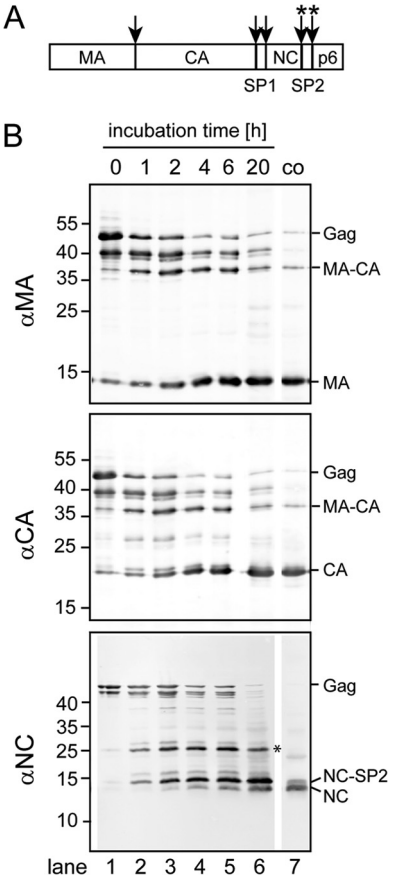


**FIG 4** Induced processing of Gag subunits. (A) Schematic drawing of the Gag polyprotein; two spacer peptides, SP1 and SP2, separate the mature subunits. Arrows indicate PR cleavage sites. Asterisks mark cleavage sites in the NC-SP2-p6 region. (B) Immunoblot analysis of Gag processing after inhibitor washout. Particles purified from virus-producing cells grown in the presence of APV were subjected to inhibitor washout and incubated at 37°C for the indicated time points. Samples were separated by SDS-PAGE, and viral proteins were detected by quantitative immunoblotting using the indicated antisera. co, control particles prepared from DMSO-treated cells. Numbers on the left of blots are molecular masses in kDa.

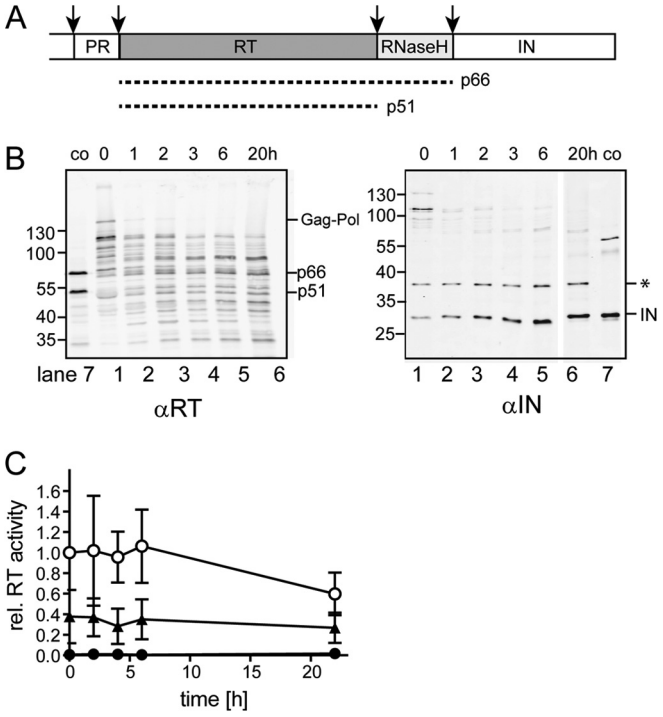


**FIG 5** Induced processing of Pol subunits. (A) Schematic drawing of the Pol polyprotein region. Arrows indicate PR cleavage sites. Dashed lines represent the p66 and p51 subunits of the mature RT heterodimer. (B) Immunoblot analysis of Gag-Pol processing after inhibitor washout. Particles purified from virus-producing cells grown in the presence of APV were subjected to inhibitor washout and incubated at 37°C for the indicated time points. Samples were separated by SDS-PAGE, and viral proteins were detected by quantitative immunoblotting using the indicated antisera. co, control particles prepared from DMSO-treated cells. Numbers on the left of gels are molecular masses in kDa. (C) Particle-associated RT activity. Virions prepared as in Fig. 2 were incubated for the indicated time points at 37°C and lysed, and RT activity of samples was determined using a PCR-enhanced RT activity assay (33). The graph shows mean values and SD from four independent experiments. Values were normalized to the respective DMSO control measured before incubation at 37°C. Open circles, DMSO control; filled triangles, APV; filled circles, SQV.

particle infectivity or virion morphogenesis (20, 21, 44), suggesting that the residual NC-SP2 is not likely to be the cause of altered capsid morphology. A complete block of both NC-SP2 and SP2-p6 processing events strongly reduces infectivity, however, and also results in a high proportion of aberrant viral core structures (20, 21, 44). Thus, residual NC-SP2-p6 could contribute to functional and structural defects in our particle preparations. Nevertheless, the relative proportion of putative NC-SP2-p6 detected is unlikely to fully explain the observed phenotype.

We extended our immunoblot analyses to the Pol region of the Gag-Pol polyprotein, which is also a substrate for PR (Fig. 5A). Cleavage of Pol appeared to be more refractory to PI-mediated inhibition of proteolysis than processing events within Gag (Fig. 5B, lane 1). Very little of the unprocessed Gag-Pol was detected directly after inhibitor washout, even without further incubation, and a number of processing products was observed. A significant proportion of fully processed IN, as well as an unidentified IN containing an ~40-kDa product (Fig. 5B, asterisk), was detected directly after washout, indicating that processing at the N terminus of IN was only partially inhibited by APV (Fig. 5B, right). Almost complete conversion to mature IN occurred within 4 to 6 h; the unidentified IN-containing product was, however, stable toward further processing.

Immunoblots using antibodies raised against RT revealed a highly aberrant protein pattern at all time points analyzed (Fig. 5B, left). The RT-reactive pattern observed for particles directly after washout confirmed the incomplete inhibition of Pol processing (as we had observed with anti-IN antiserum), with most of the bands migrating at lower molecular mass than the Gag-Pol precursor (Fig. 5B, left, lane 1). The vast majority of the detected products at this time point did not correspond to the fully processed RT subunits p66 and p51 found in mature control particles (Fig. 5B, left, lane 7). A complex band pattern, including products migrating below 51 kDa, indicated cleavage at off-target positions already after the washout procedure. Incubation at 37°C following PI washout resulted in shift of the band pattern toward lower-molecular-mass products, again not corresponding to expected processing intermediates or end products. Prolonged incubation under PR activation conditions (Fig. 5B, left, lane 6) still yielded a complex pattern of products, with only a minute proportion po-

Downloaded from http://jvi.asm.org/ on November 6, 2014 by Uppsala Univ BMC

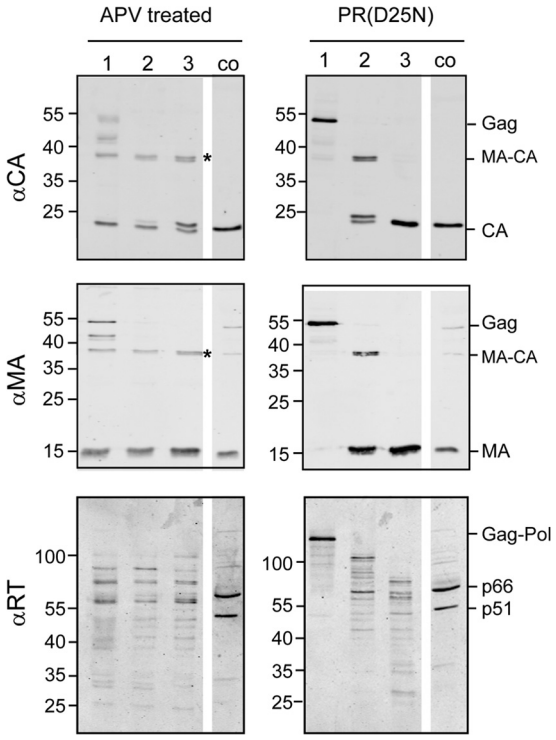


**FIG 6** Processing of virion-derived polyproteins by exogenous HIV-1 PR. Immature virions purified by ultracentrifugation from the supernatant of cells transfected with pCHIV and grown in the presence of APV (left) or transfected with the PR-defective variant pCHIV(D25N) (right) were incubated at pH 6.0 for 6 h (lanes 1). Subsequently, particles were lysed using 0.1% TX-100 and incubated with purified recombinant HIV-1 PR at 37°C for 1 h at an ~20:1 (lane 2) or 4:1 (lane 3) molar ratio of Gag to PR. Samples were separated by SDS-PAGE, and viral proteins were detected by quantitative immunoblot using the indicated antisera. co, control particles from DMSO-treated cells. Positions of marker proteins (molecular masses in kDa) are indicated to the left, and positions of Gag processing products or mature RT subunits are indicated to the right.

tentially attributable to the regular p66 and p51 RT subunits and a significant proportion of products smaller than p51.

This finding prompted us to test RT enzymatic activity associated with particle preparations (Fig. 5C), since full activity depends on formation of the mature p66/p51 heterodimer. In agreement with the incomplete inhibition of Pol processing, a low level of RT activity was detected in virions produced in the presence of APV (Fig. 5C, filled triangles), while virions generated in the presence of SQV lacked detectable activity (Fig. 5C, filled circles). Incubation after PI washout did not restore RT activity for either SQV- or APV-treated samples, however. No increase in RT activity was observed, in line with the observed processing patterns and the lack of recovery of virion infectivity.

**Cleavage of Gag and Gag-Pol by exogenous PR.** Incorrect processing of RT within the assembled particle might arise from insufficient PR enzymatic activity recovered, from failure of Pol to present as an appropriate substrate in this context, or both. Furthermore, particles prepared in the presence of APV contained small amounts of the Gag-Pol precursor already at the time of washout (Fig. 5B, left), and the partially (and probably aberrantly) cleaved products observed might not be correctly recognized as a substrate for the generation of the regular p66/p51 RT heterodimer. To address these issues, we incubated lysed particles after washout with purified recombinant HIV-1 PR in *trans*. Particles prepared in the presence of APV (Fig. 6, left) or carrying an inactivating mutation in the PR active site (D25N; Fig. 6, right) were subjected to washout and incubation at 37°C for 6 h (Fig. 6, lane 1). Subsequently, the viral membrane was disrupted with detergent, and different amounts of purified recombinant HIV-1 PR were added with continued incubation for 1 h at 37°C (lanes 2 and 3). The addition of PR to lysed particles carrying an inactive PR(D25N) led to concentration-dependent processing of Gag to its mature MA and CA subunits, while processing of Gag-Pol was aberrant, with little, if any, regular p66/p51 RT heterodimer produced (Fig. 6, right, lanes 2 and 3). Production of mature MA and CA was also observed upon PR treatment of APV-treated particles following washout and partial proteolysis, but some intermediate product appeared to be refractory to exogenous PR cleavage (Fig. 6, left, asterisk). As in the previous experiments, RT-reactive products appeared aberrant after APV washout and incubation (Fig. 6, left, lane 1). Exogenous PR did not convert these products into mature p66/p51, and most of the "prematured" products appeared to be refractory to further cleavage (Fig. 6, left, lanes 2 and 3).

## DISCUSSION

The results presented here demonstrate that HIV-1 PR activation *in situ* can be achieved by an inhibitor washout strategy, leading to efficient processing of Gag and disassembly of the immature Gag lattice. The detection of a particle with clear wt mature morphology (Fig. 3Avii), as well as of particles with only mildly aberrant architecture, indicates that the process of HIV-1 maturation can in principle be reconstituted by induced PR activation. However, induced polyprotein processing did not restore HIV-1 infectivity, and the majority of particles displayed anomalous capsid structures and highly irregular RT processing patterns with concomitant lack of RT activity.

The efficiency of the washout procedure correlated with previously determined off-rates of the respective compound rather than with their inhibitory constants. We presume that during the washout procedure, the inhibitor dissociates from the enzyme-inhibitor complex following the first-order kinetics described by the kinetic rate constant of the dissociation reaction.

Complete CA processing was observed only after 20 to 24 h, however, with a $t_{1/2}$ for Gag polyprotein processing of ~5 h in the optimal case of APV. Although the true time course of HIV-1 maturation is currently unknown, electron micrographs of virus-producing cells show mainly clearly mature or immature particles in the vicinity of the plasma membrane, and morphologically mature particles apparently captured on the micrograph during transfer from producing to new target cell are easily detected in the confined space of virological synapses (45, 46). Based on these observations and on a comprehensive model of HIV-1 maturation derived from integrating available *in vitro* data (47), we argue that Gag maturation within the nascent virion should occur considerably faster than what was observed in the current study. Slow maturation over 6 h during endocytotic uptake was reported earlier (48), but these results are in conflict with many other reports and are not likely to reflect the true kinetics of HIV-1 maturation. The tight binding of PI in general, resulting in a slow time course of induced proteolysis even under optimal conditions, may thus be a limitation inherent to our approach.

Downloaded from http://jvi.asm.org/ on November 6, 2014 by Uppsala Univ BMC

The apparently delayed kinetics of processing upon washout, which might also differentially affect cleavage at individual sites, can explain aberrant maturation leading to noninfectious particles. Two major defects were observed in this study: (i) irregular capsid morphology and (ii) aberrant processing of the RT region of Gag-Pol with concomitant lack of RT activity. Both defects are individually sufficient to explain the lack of infectivity of particles recovered from induced maturation: regular capsid morphology has been shown to be important for early HIV-1 replication, and RT activity is essential to form the proviral cDNA to be integrated into the host cell genome. The two phenotypes may either be functionally linked (e.g., through rearrangement of Gag-Pol dimers within the immature particle over time or through aberrant RNP formation in the absence of RT; see below) or may constitute independent consequences of an altered time course of polyprotein processing. Arguments for either hypothesis can be derived from previous studies, and further experiments will be needed to clarify this question.

Mutational studies had revealed that blocking cleavage sites downstream of CA can affect formation of mature HIV-1 cores, even though CA is fully converted into the mature form (20, 21). In particular, rapid separation between the NC and p6 domains appears to be critical. Residual amounts of an intermediate likely corresponding to NC-SP2-p6 detected in our preparations indicate that this separation may be impaired under inhibitor washout conditions. Data from mutational analyses suggest that tight temporal control of processing at individual sites is required in order to correlate RNP condensation with mature capsid assembly. A crucial importance of NC-SP2-p6 processing dynamics is also implied by the mapping of resistance-associated mutations restoring viral fitness in PI-resistant HIV-1 to this region (49). Failure to faithfully reconstitute wt processing kinetics may thus result in aberrant particle morphology. Furthermore, small amounts of noncleavable Gag derivatives have been shown to exert a *trans*-dominant negative effect on HIV-1 maturation and infectivity (44, 50). The delayed processing kinetics we observed also result in prolonged coexistence of intermediates and end products at very high concentrations within the confined space of a virion, and it appears likely these may contribute to, or cause, morphologically aberrant capsids.

A high proportion of particles obtained by inhibitor washout displayed an RNP outside a capsid structure. Condensed RNP adjacent to empty capsid structures is also characteristic for HIV-1 lacking IN or carrying IN point mutations affecting steps other than integration (class II IN mutations) (51; reviewed in reference 52). Furthermore, an "empty capsid" phenotype is frequently observed for HIV-1 particles prepared in the presence of various allosteric IN inhibitors (53–55). It has been speculated that IN aggregates within the virion promoted by these compounds interfere with mature particle formation (reviewed in reference 56), but their binding to the IN domain might also change the architecture and/or oligomerization of particle-associated Gag-Pol. Seen in this light, our detection of nonencapsidated RNPs in combination with the observed instability of Gag-Pol suggests to us that rearrangement of Gag-Pol molecules during maturation may play a role in RNP encapsidation and core morphology.

The RT region appeared particularly sensitive to changes in the timing and/or dynamics of proteolysis, and correct processing could not be achieved (even at high concentrations of exogenous PR) when assembled Gag/Gag-Pol lattices were presented as the substrate. This suggests that Gag-Pol rearrangement during the assembly, budding, and/or maturation process modifies the susceptibility of the RT domain for PR. This interpretation may be supported by results from published HIV-1 mutational analyses, showing that formation of the mature RT p66/p51 subunits is highly sensitive to mutations affecting RT dimer stability and/or cleavage at the RT-RNaseH processing site. In particular, point mutations in the RT thumb domain or in the RT-RNaseH linker region often result in Gag-Pol degradation (57, 58), resembling the pattern observed in this study. Currently, nothing is known about the arrangement and structure of Gag-Pol molecules or Gag-Pol dimer stability in the immature virion. However, studies using purified RT domains *in vitro* revealed that p66/p66 homodimers are considerably less stable than the fully processed p66/p51 heterodimer (59). Delayed conversion of RT into the stable heterodimeric form under washout conditions could thus result in exposure of monomeric RT domains prone to degradation in the presence of equimolar concentrations of PR in the confined environment of the particle.

Based on the results obtained here, we conclude that induced maturation by inhibitor washout is possible in principle; however, more rapid PR activation triggered at an appropriate time point with respect to particle assembly is likely critical for faithful HIV-1 maturation and recovery of infectivity. Apparently, the relatively slow procedure of inhibitor washout, performed with variable delay after immature particle assembly, does not fulfill these criteria. Faster and more targeted induction of the maturation process could be accomplished by employing a photolabile inhibitor allowing light-induced PR activation *in situ*. Experiments toward the generation and characterization of such a tool are under way, and we expect that these studies will further enhance our understanding of the complex process of HIV-1 maturation.

## ACKNOWLEDGMENTS

Protease inhibitors were obtained through the AIDS Research and Reference Reagent Program, Division of AIDS, NIAID.

This work was supported by a grant from the Deutsche Forschungsgemeinschaft to B.M. (MU885-5/1). Work in the Briggs lab is supported by the Chica und Heinz Schaller Stiftung. J.K. was supported by the Ministry of Education of the Czech Republic, grant no. P208-12-G016. H.-G.K. and B.M. are investigators of the CellNetworks Cluster of Excellence (EXC81).

## REFERENCES

1. **Briggs JA, Krausslich HG.** 2011. The molecular architecture of HIV. J. Mol. Biol. **410:**491–500. http://dx.doi.org/10.1016/j.jmb.2011.04.021.
2. **Ganser-Pornillos BK, Yeager M, Pornillos O.** 2012. Assembly and architecture of HIV. Adv. Exp. Med. Biol. **726:**441–465. http://dx.doi.org/10.1007/978-1-4614-0980-9_20.
3. **Sundquist WI, Krausslich HG.** 2012. HIV-1 assembly, budding, and maturation. Cold Spring Harb. Perspect. Med. **2:**a006924. http://dx.doi.org/10.1101/cshperspect.a006924.
4. **Anderson J, Schiffer C, Lee SK, Swanstrom R.** 2009. Viral protease inhibitors. Handb. Exp. Pharmacol. **2009**(189):85–110. http://dx.doi.org/10.1007/978-3-540-79086-0_4.
5. **Pokorna J, Machala L, Rezacova P, Konvalinka J.** 2009. Current and novel inhibitors of HIV protease. Viruses **1:**1209–1239. http://dx.doi.org/10.3390/v1031209.
6. **Wensing AM, van Maarseveen NM, Nijhuis M.** 2010. Fifteen years of HIV protease inhibitors: raising the barrier to resistance. Antiviral Res. **85:**59–74. http://dx.doi.org/10.1016/j.antiviral.2009.10.003.
7. **Benjamin J, Ganser-Pornillos BK, Tivol WF, Sundquist WI, Jensen GJ.** 2005. Three-dimensional structure of HIV-1 virus-like particles by electron cryotomography. J. Mol. Biol. **346:**577–588. http://dx.doi.org/10.1016/j.jmb.2004.11.064.

Downloaded from http://jvi.asm.org/ on November 6, 2014 by Uppsala Univ BMC

8. **Briggs JA, Riches JD, Glass B, Bartonova V, Zanetti G, Krausslich HG.** 2009. Structure and assembly of immature HIV. Proc. Natl. Acad. Sci. U. S. A. **106:**11090–11095. http://dx.doi.org/10.1073/pnas.0903535106.
9. **Briggs JA, Grunewald K, Glass B, Forster F, Krausslich HG, Fuller SD.** 2006. The mechanism of HIV-1 core assembly: insights from three-dimensional reconstructions of authentic virions. Structure **14:**15–20. http://dx.doi.org/10.1016/j.str.2005.09.010.
10. **Briggs JA, Wilk T, Welker R, Krausslich HG, Fuller SD.** 2003. Structural organization of authentic, mature HIV-1 virions and cores. EMBO J. **22:** 1707–1715. http://dx.doi.org/10.1093/emboj/cdg143.
11. **Wright ER, Schooler JB, Ding HJ, Kieffer C, Fillmore C, Sundquist WI, Jensen GJ.** 2007. Electron cryotomography of immature HIV-1 virions reveals the structure of the CA and SP1 Gag shells. EMBO J. **26:**2218–2226. http://dx.doi.org/10.1038/sj.emboj.7601664.
12. **Ganser BK, Li S, Klishko VY, Finch JT, Sundquist WI.** 1999. Assembly and analysis of conical models for the HIV-1 core. Science **283:**80–83. http://dx.doi.org/10.1126/science.283.5398.80.
13. **Li S, Hill CP, Sundquist WI, Finch JT.** 2000. Image reconstructions of helical assemblies of the HIV-1 CA protein. Nature **407:**409–413. http://dx.doi.org/10.1038/35030177.
14. **Bharat TA, Davey NE, Ulbrich P, Riches JD, de Marco A, Rumlova M, Sachse C, Ruml T, Briggs JA.** 2012. Structure of the immature retroviral capsid at 8 A resolution by cryo-electron microscopy. Nature **487:**385–389. http://dx.doi.org/10.1038/nature11169.
15. **Lanman J, Lam TT, Emmett MR, Marshall AG, Sakalian M, Prevelige PE, Jr.** 2004. Key interactions in HIV-1 maturation identified by hydrogen-deuterium exchange. Nat. Struct. Mol. Biol. **11:**676–677. http://dx.doi.org/10.1038/nsmb790.
16. **Krausslich HG.** 1991. Human immunodeficiency virus proteinase dimer as component of the viral polyprotein prevents particle assembly and viral infectivity. Proc. Natl. Acad. Sci. U. S. A. **88:**3213–3217. http://dx.doi.org/10.1073/pnas.88.8.3213.
17. **Erickson-Viitanen S, Manfredi J, Viitanen P, Tribe DE, Tritch R, Hutchison CA, III, Loeb DD, Swanstrom R.** 1989. Cleavage of HIV-1 Gag polyprotein synthesized *in vitro*: sequential cleavage by the viral protease. AIDS Res. Human Retroviruses **5:**577–591. http://dx.doi.org/10.1089/aid.1989.5.577.
18. **Pettit SC, Lindquist JN, Kaplan AH, Swanstrom R.** 2005. Processing sites in the human immunodeficiency virus type 1 (HIV-1) Gag-Pro-Pol precursor are cleaved by the viral protease at different rates. Retrovirology **2:**66. http://dx.doi.org/10.1186/1742-4690-2-66.
19. **Pettit SC, Moody MD, Wehbie RS, Kaplan AH, Nantermet PV, Klein CA, Swanstrom R.** 1994. The p2 domain of human immunodeficiency virus type 1 Gag regulates sequential proteolytic processing and is required to produce fully infectious virions. J. Virol. **68:**8017–8027.
20. **Coren LV, Thomas JA, Chertova E, Sowder RC, II, Gagliardi TD, Gorelick RJ, Ott DE.** 2007. Mutational analysis of the C-terminal gag cleavage sites in human immunodeficiency virus type 1. J. Virol. **81:** 10047–10054. http://dx.doi.org/10.1128/JVI.02496-06.
21. **de Marco A, Heuser AM, Glass B, Krausslich HG, Muller B, Briggs JA.** 2012. Role of the SP2 domain and its proteolytic cleavage in HIV-1 structural maturation and infectivity. J. Virol. **86:**13708–13716. http://dx.doi.org/10.1128/JVI.01704-12.
22. **Wiegers K, Rutter G, Kottler H, Tessmer U, Hohenberg H, Krausslich HG.** 1998. Sequential steps in human immunodeficiency virus particle maturation revealed by alterations of individual Gag polyprotein cleavage sites. J. Virol. **72:**2846–2854.
23. **Lee SK, Potempa M, Swanstrom R.** 2012. The choreography of HIV-1 proteolytic processing and virion assembly. J. Biol. Chem. **287:**40867–40874. http://dx.doi.org/10.1074/jbc.R112.399444.
24. **Chojnacki J, Muller B.** 2013. Investigation of HIV-1 assembly and release using modern fluorescence imaging techniques. Traffic **14:**15–24. http://dx.doi.org/10.1111/tra.12006.
25. **Lata R, Conway JF, Cheng N, Duda RL, Hendrix RW, Wikoff WR, Johnson JE, Tsuruta H, Steven AC.** 2000. Maturation dynamics of a viral capsid: visualization of transitional intermediate states. Cell **100:**253–263. http://dx.doi.org/10.1016/S0092-8674(00)81563-9.
26. **Steven AC, Heymann JB, Cheng N, Trus BL, Conway JF.** 2005. Virus maturation: dynamics and mechanism of a stabilizing structural transition that leads to infectivity. Curr. Opin. Struct. Biol. **15:**227–236. http://dx.doi.org/10.1016/j.sbi.2005.03.008.
27. **Manchester M, Loeb DD, Everitt L, Moody M, Hutchison CA, III, Swanstrom R.** 1991. Analysis of temperature-sensitive mutants of the HIV-1 protease. Adv. Exp. Med. Biol. **306:**493–497. http://dx.doi.org/10.1007/978-1-4684-6012-4_63.
28. **Konvalinka J.** 1994. Structural and molecular biology of protease function and inhibition. Keystone Symposium. Santa Fe, New Mexico, March 5–12, 1994. Abstracts. J. Cell. Biochem. Suppl. **18D:**117–177.
29. **Sluis-Cremer N, Arion D, Abram ME, Parniak MA.** 2004. Proteolytic processing of an HIV-1 pol polyprotein precursor: insights into the mechanism of reverse transcriptase p66/p51 heterodimer formation. Int. J. Biochem. Cell Biol. **36:**1836–1847. http://dx.doi.org/10.1016/j.biocel.2004.02.020.
30. **Adachi A, Koenig S, Gendelman HE, Daugherty D, Gattoni-Celli S, Fauci AS, Martin MA.** 1987. Productive, persistent infection of human colorectal cell lines with human immunodeficiency virus. J. Virol. **61:**209–213.
31. **Lampe M, Briggs JA, Endress T, Glass B, Riegelsberger S, Krausslich HG, Lamb DC, Brauchle C, Muller B.** 2007. Double-labeled HIV-1 particles for study of virus-cell interaction. Virology **360:**92–104. http://dx.doi.org/10.1016/j.virol.2006.10.005.
32. **Dettenhofer M, Yu XF.** 1999. Proline residues in human immunodeficiency virus type 1 p6(Gag) exert a cell type-dependent effect on viral replication and virion incorporation of Pol proteins. J. Virol. **73:**4696–4704.
33. **Pizzato M, Erlwein O, Bonsall D, Kaye S, Muir D, McClure MO.** 2009. A one-step SYBR green I-based product-enhanced reverse transcriptase assay for the quantitation of retroviruses in cell culture supernatants. J. Virol. Methods **156:**1–7. http://dx.doi.org/10.1016/j.jviromet.2008.10.012.
34. **Mastronarde DN.** 2005. Automated electron microscope tomography using robust prediction of specimen movements. J. Struct. Biol. **152:**36–51. http://dx.doi.org/10.1016/j.jsb.2005.07.007.
35. **Kremer JR, Mastronarde DN, McIntosh JR.** 1996. Computer visualization of three-dimensional image data using IMOD. J. Struct. Biol. **116:**71–76. http://dx.doi.org/10.1006/jsbi.1996.0013.
36. **Dierynck I, De Wit M, Gustin E, Keuleers I, Vandersmissen J, Hallenberger S, Hertogs K.** 2007. Binding kinetics of darunavir to human immunodeficiency virus type 1 protease explain the potent antiviral activity and high genetic barrier. J. Virol. **81:**13845–13851. http://dx.doi.org/10.1128/JVI.01184-07.
37. **Markgren PO, Schaal W, Hamalainen M, Karlen A, Hallberg A, Samuelsson B, Danielson UH.** 2002. Relationships between structure and interaction kinetics for HIV-1 protease inhibitors. J. Med. Chem. **45:**5430–5439. http://dx.doi.org/10.1021/jm0208370.
38. **Shuman CF, Hamalainen MD, Danielson UH.** 2004. Kinetic and thermodynamic characterization of HIV-1 protease inhibitors. J. Mol. Recognit. **17:**106–119. http://dx.doi.org/10.1002/jmr.655.
39. **Darke PL, Leu CT, Davis LJ, Heimbach JC, Diehl RE, Hill WS, Dixon RA, Sigal IS.** 1989. Human immunodeficiency virus protease. Bacterial expression and characterization of the purified aspartic protease. J. Biol. Chem. **264:**2307–2312.
40. **Hyland LJ, Tomaszek TA, Jr, Meek TD.** 1991. Human immunodeficiency virus-1 protease. 2. Use of pH rate studies and solvent kinetic isotope effects to elucidate details of chemical mechanism. Biochemistry **30:** 8454–8463.
41. **Polgar L, Szeltner Z, Boros I.** 1994. Substrate-dependent mechanisms in the catalysis of human immunodeficiency virus protease. Biochemistry **33:**9351–9357. http://dx.doi.org/10.1021/bi00197a040.
42. **Lee SK, Potempa M, Kolli M, Ozen A, Schiffer CA, Swanstrom R.** 2012. Context surrounding processing sites is crucial in determining cleavage rate of a subset of processing sites in HIV-1 Gag and Gag-Pro-Pol polyprotein precursors by viral protease. J. Biol. Chem. **287:**13279–13290. http://dx.doi.org/10.1074/jbc.M112.339374.
43. **Konvalinka J, Heuser AM, Hruskova-Heidingsfeldova O, Vogt VM, Sedlacek J, Strop P, Krausslich HG.** 1995. Proteolytic processing of particle-associated retroviral polyproteins by homologous and heterologous viral proteinases. Eur. J. Biochem. **228:**191–198. http://dx.doi.org/10.1111/j.1432-1033.1995.tb20249.x.
44. **Muller B, Anders M, Akiyama H, Welsch S, Glass B, Nikovics K, Clavel F, Tervo HM, Keppler OT, Krausslich HG.** 2009. HIV-1 Gag processing intermediates trans-dominantly interfere with HIV-1 infectivity. J. Biol. Chem. **284:**29692–29703. http://dx.doi.org/10.1074/jbc.M109.027144.
45. **Jolly C, Welsch S, Michor S, Sattentau QJ.** 2011. The regulated secretory pathway in CD4(+) T cells contributes to human immunodeficiency virus type-1 cell-to-cell spread at the virological synapse. PLoS Pathog. **7:**e1002226. http://dx.doi.org/10.1371/journal.ppat.1002226.


Downloaded from http://jvi.asm.org/ on November 6, 2014 by Uppsala Univ BMC

46. **Martin N, Welsch S, Jolly C, Briggs JA, Vaux D, Sattentau QJ.** 2010. Virological synapse-mediated spread of human immunodeficiency virus type 1 between T cells is sensitive to entry inhibition. J. Virol. **84:**3516–3527. http://dx.doi.org/10.1128/JVI.02651-09.
47. **Konnyu B, Sadiq SK, Turanyi T, Hirmondo R, Muller B, Krausslich HG, Coveney PV, Muller V.** 2013. Gag-Pol processing during HIV-1 virion maturation: a systems biology approach. PLoS Comput. Biol. **9:**e1003103. http://dx.doi.org/10.1371/journal.pcbi.1003103.
48. **Dale BM, McNerney GP, Thompson DL, Hubner W, de Los Reyes K, Chuang FY, Huser T, Chen BK.** 2011. Cell-to-cell transfer of HIV-1 via virological synapses leads to endosomal virion maturation that activates viral membrane fusion. Cell Host Microbe **10:**551–562. http://dx.doi.org/10.1016/j.chom.2011.10.015.
49. **Nijhuis M, van Maarseveen NM, Lastere S, Schipper P, Coakley E, Glass B, Rovenska M, de Jong D, Chappey C, Goedegebuure IW, Heilek-Snyder G, Dulude D, Cammack N, Brakier-Gingras L, Konvalinka J, Parkin N, Krausslich HG, Brun-Vezinet F, Boucher CA.** 2007. A novel substrate-based HIV-1 protease inhibitor drug resistance mechanism. PLoS Med. **4:**e36. http://dx.doi.org/10.1371/journal.pmed.0040036.
50. **Lee SK, Harris J, Swanstrom R.** 2009. A strongly transdominant mutation in the human immunodeficiency virus type 1 *gag* gene defines an Achilles heel in the virus life cycle. J. Virol. **83:**8536–8543. http://dx.doi.org/10.1128/JVI.00317-09.
51. **Engelman A, Englund G, Orenstein JM, Martin MA, Craigie R.** 1995. Multiple effects of mutations in human immunodeficiency virus type 1 integrase on viral replication. J. Virol. **69:**2729–2736.
52. **Engelman A.** 1999. *In vivo* analysis of retroviral integrase structure and function. Adv. Virus Res. **52:**411–426. http://dx.doi.org/10.1016/S0065-3527(08)60309-7.
53. **Jurado KA, Wang H, Slaughter A, Feng L, Kessl JJ, Koh Y, Wang W, Ballandras-Colas A, Patel PA, Fuchs JR, Kvaratskhelia M, Engelman A.** 2013. Allosteric integrase inhibitor potency is determined through the inhibition of HIV-1 particle maturation. Proc. Natl. Acad. Sci. U. S. A. **110:**8690–8695. http://dx.doi.org/10.1073/pnas.1300703110.
54. **Balakrishnan M, Yant SR, Tsai L, O'Sullivan C, Bam RA, Tsai A, Niedziela-Majka A, Stray KM, Sakowicz R, Cihlar T.** 2013. Non-catalytic site HIV-1 integrase inhibitors disrupt core maturation and induce a reverse transcription block in target cells. PLoS One **8:**e74163. http://dx.doi.org/10.1371/journal.pone.0074163.
55. **Desimmie BA, Schrijvers R, Demeulemeester J, Borrenberghs D, Weydert C, Thys W, Vets S, Van Remoortel B, Hofkens J, De Rijck J, Hendrix J, Bannert N, Gijsbers R, Christ F, Debyser Z.** 2013. LEDGINs inhibit late stage HIV-1 replication by modulating integrase multimerization in the virions. Retrovirology **10:**57. http://dx.doi.org/10.1186/1742-4690-10-57.
56. **Jurado KA, Engelman A.** 2013. Multimodal mechanism of action of allosteric HIV-1 integrase inhibitors. Exp. Rev. Mol. Med. **15:**e14. http://dx.doi.org/10.1017/erm.2013.15.
57. **Abram ME, Parniak MA.** 2005. Virion instability of human immunodeficiency virus type 1 reverse transcriptase (RT) mutated in the protease cleavage site between RT p51 and the RT RNase H domain. J. Virol. **79:**11952–11961. http://dx.doi.org/10.1128/JVI.79.18.11952-11961.2005.
58. **Dunn LL, McWilliams MJ, Das K, Arnold E, Hughes SH.** 2009. Mutations in the thumb allow human immunodeficiency virus type 1 reverse transcriptase to be cleaved by protease in virions. J. Virol. **83:**12336–12344. http://dx.doi.org/10.1128/JVI.00676-09.
59. **Restle T, Muller B, Goody RS.** 1990. Dimerization of human immunodeficiency virus type 1 reverse transcriptase. A target for chemotherapeutic intervention. J. Biol. Chem. **265:**8986–8988.


Downloaded from http://jvi.asm.org/ on November 6, 2014 by Uppsala Univ BMC